

Some Limitations on the Detection of High Elongational Stress Effects in Dilute Polymer Solutions

R. Y. TING and D. L. HUNSTON, *Naval Research Laboratory, Chemistry Division, Code 6170, Washington, D.C. 20375*

Synopsis

The elongational flow behavior of dilute polymer solutions is of great current interest because it has been suggested that elongational viscosity effects may be involved in a number of phenomena such as turbulent drag reduction and flow cavitation suppression. Unfortunately, recent experiments, in trying to investigate elongational effects, have produced widely varying results. In this paper, an attempt is made to analyze one of the factors that contribute to this diversity. By using a generalized convected Maxwell model, it is shown that in a transient elongational flow, both stretching rate and flow time must reach the proper values before high stress levels can be observed. This is true for both accelerating flows such as through a cone or wedge and decelerating flows such as in a free jet. Since most previous experiments have not considered flow time, consistent results cannot be expected. Consequently, the proper control of all flow conditions is an essential requirement when trying to observe high stress levels. The results presented here provide valuable guidelines in this regard.

INTRODUCTION

The importance of polymer response to elongational flows is well known in certain aspects of polymer processing such as extrusion. In recent years, the behavior of solutions in elongational flow has also stimulated a great deal of interest because it has been associated with a number of important phenomena observed in dilute polymer solutions. Recent experiments have revealed many such effects. For example, the addition of small amounts of certain high molecular weight polymers to a solvent has been shown to reduce the frictional drag associated with turbulent pipe flows.¹ Likewise, polymeric additives can affect the energy transport process and result in a reduction of the turbulent heat transfer coefficient.² Even in laminar flows, the addition of polymers can alter the streamline patterns around objects.³ Other experiments have shown that the stress effect of macromolecules can suppress flow-generated cavitation by as much as 60% when compared with that in water.⁴ Similar inhibition effects have been reported in jet cavitation and venturi cavitation as well.⁵ Finally, the characteristics for the generation of flow-induced instabilities at a compliant coating/fluid interface^{6,7} and for the breakup of fluid jets^{8,9} are altered by the addition of polymer. It is clear, therefore, that such additives can affect flow behavior in many ways.

Despite the great diversity of these effects, recent work has revealed a definite pattern involving some unique characteristics common to all. This has led to the speculation that an analysis of these similarities may eventually produce a unified theory to satisfactorily explain many aspects of the phenomena. Perhaps the most striking similarity is that only very small amounts of polymer are needed to produce substantial alterations in flow behavior. For example, concentrations as low as a few parts per million by weight can give large reductions in turbulent drag and cavitation.^{1,4} The second important similarity concerns the nature of the deformation patterns. An analysis of the flows involved in these phenomena indicates that deformations of an axisymmetric stretching or compression are present. In the cases of jet or venturi flows⁵ and flows approaching the stagnation point of a blunt-nosed object,^{3,4} the existence of such deformation fields is quite evident. In the cases of wall turbulence such as that in pipe flows, recent flow visualization studies^{10,11} have indicated that turbulence generation is closely related to the turbulent bursting process, which was found to contain fluid motions of a stretching nature. In fact, experimental observations¹² have shown that polymeric additives suppress such activities in the wall region of the turbulent boundary layer.

The importance of this stretching or elongational-type motion was first recognized by Peterlin,¹³ Metzner,¹⁴ and Lumley^{15,16} who noted that theoretical models for polymer rheology predicted that the addition of very small amounts of polymer to a solvent would produce large increases in the resistance to steady-state elongational flow. Several more recent theoretical analyses¹⁷⁻¹⁹ have suggested that this is also true for transient flows. For example, Lumley²⁰ has tried to model the behavior of dilute polymer solutions in turbulent flow. His studies suggest that under the proper conditions, the elongational motions present in the flow can produce large extensions of the polymer molecules. As a result of these studies and other similar work, it has been proposed that a mechanism involving elongational viscosity might explain many of the anomalous effects observed in dilute polymer solutions. In an effort to clarify this point, a number of workers have studied converging flows in an attempt to experimentally verify the theoretical predictions regarding the behavior of dilute polymer solutions in elongational flow. Unfortunately, these studies have produced widely varied results. In some cases, the elongational viscosity was found to be very large^{21,22} and the polymer molecules highly extended.²³ In other experiments, neither of these effects was observed.^{24,25} Consequently, the objective in this paper is to analyze one of the difficulties involved in studies of this type and to indicate how the experimental conditions can be adjusted to optimize the chances for obtaining positive results.

MODEL AND ELONGATIONAL VISCOSITY

Elaborate molecular theories, such as that of Rouse,²⁶ have been developed to model the motions of isolated polymer molecules. By employing such models, authors like Peterlin²⁷ have studied the dependence of polymer intrinsic viscosity and other properties on the hydrodynamic flow fields. These papers indicate that in a steady flow field with a longitudinal gradient, the extension of the polymer molecules is much greater than that obtained with a transverse gradient. The stress levels required to maintain this extension are very high even at low

polymer concentrations. It was later pointed out, however, that, although the steady-state stress levels may be large, the transient behavior can be quite different.²⁸ Recent investigations have, therefore, proposed constitutive equations which are more adaptable to the treatment of transient flows.¹⁷⁻¹⁹ Such a model will be used for the discussion presented here. In this continuum model,¹⁹ which is based on the bead-spring molecular theories of Rouse and Zimm, the total stress σ is related to the strain rate tensor \mathbf{d} by

$$\sigma = -p\mathbf{I} + \eta_s \mathbf{d} + \sum_1^m \sigma^{(n)} \quad (1)$$

where p is the hydrostatic pressure, η_s is the solvent viscosity, and $\sigma^{(n)}$ is the n th mode stress deviator satisfying

$$\sigma^{(n)} + \lambda_n \frac{D\sigma^{(n)}}{Dt} = \eta_n \mathbf{d} \quad (2)$$

In eq. (2), the convected material derivatives are used;²⁹ λ_n is the n th relaxation time and η_n is the contribution of the n th mode to zero-shear solution viscosity. Values for these parameters can be obtained from the appropriate molecular theory such as that of Rouse.^{19,26}

For an elongational deformation with constant stretching rate Γ , the strain tensor \mathbf{d} is

$$\mathbf{d} = \begin{bmatrix} 2\Gamma & 0 & 0 \\ 0 & -\Gamma & 0 \\ 0 & 0 & -\Gamma \end{bmatrix} \quad (3)$$

The elongational stress effect is presented in terms of a parameter $\bar{\eta}$, called the reduced elongational viscosity,

$$\bar{\eta} = \frac{\sigma_{11} - \sigma_{22}}{\eta_s \Gamma} \quad (4)$$

For the model used here,

$$\bar{\eta} = 3 + \sum_1^m \left\{ \frac{2cRT\lambda_n}{M_w \eta_s (1 - 2\lambda_n \Gamma)} \left[1 - \exp\left(-\frac{1 - 2\lambda_n \Gamma}{\lambda_n} t\right) \right] + \frac{cRT\lambda_n}{M_w \eta_s (1 + \lambda_n \Gamma)} \left[1 - \exp\left(-\frac{1 + \lambda_n \Gamma}{\lambda_n} t\right) \right] \right\} \quad (5)$$

where c is the polymer concentration, R is the gas constant, T is the absolute temperature, M_w is the molecular weight, and t is the physical flow time. In this equation, it is clear that as polymer concentration c approaches zero, the classical Trouton ratio for Newtonian fluids, $\bar{\eta}_N = 3$, is recovered.³⁰ For polymer solutions in steady-state flow ($t \rightarrow \infty$), the reduced elongational viscosity approaches

$$\bar{\eta} = 3 \left\{ 1 + \frac{cRT}{M_w \eta_s} \sum_1^m \frac{\lambda_n}{(1 - 2\lambda_n \Gamma)(1 + \lambda_n \Gamma)} \right\}$$

This equation shows that $\bar{\eta}$ increases rapidly with increasing stretching rate Γ , and, as expected, it approaches infinity as $(1 - 2\lambda_1 \Gamma) \rightarrow 0$. In the case of compression ($\Gamma < 0$), similar behavior is found, except that the singularity for infinite

$\bar{\eta}$ is shifted to $(1 + \lambda_1\Gamma) \rightarrow 0$. Consequently, this model gives the expected results for steady-state motion.

What is more interesting, however, is that the behavior for transient flows can also be predicted from eq. (5). The importance of this can best be illustrated by considering a specific example. Calculations¹⁹ based on eq. (5) were carried out for a 100-ppm solution of Polyox-WSR-301 (Union Carbide, $M_w \approx 2.4 \times 10^6$, $\eta = 1.21$ cP).

The results are presented in Figure 1, where curves representing contours of constant $\bar{\eta}$ at ten different values ranging from 3.1 to 10^4 are plotted in a phase plane of normalized flow time (t/λ_1) and normalized stretching rate ($\lambda_1\Gamma$). The upper portion of Figure 1 shows the results for stretching ($\Gamma > 0$), whereas the lower portion gives the curves for compression ($\Gamma < 0$). It can be seen from this figure that once the elongational flow is established, it must be maintained for a definite period of time before a given value of $\bar{\eta}$ is obtained; that is, a finite time is required for the polymer molecules to respond to the flow. For small values of $\bar{\eta}$, those close to the Trouton ratio of 3.0, the necessary flow time can be reached even when Γ is very small. For example, $\bar{\eta}$ will reach or exceed 3.1 regardless of the stretching rate at a flow time of approximately $t/\lambda_1 = 0.022$. It is also interesting to note from Figure 1 that the $\bar{\eta}$ contours exhibit a maximum in t . Consider, for instance, the case of $\bar{\eta} = 3.4$; there is a maximum in flow time ($t/\lambda_1 \approx 0.7$) at $\lambda_1\Gamma \approx -1.0$. This type of behavior becomes increasingly important as higher and higher values of $\bar{\eta}$ are considered, since the maximum becomes more pronounced and eventually approaches infinity. This can be seen in Figure 1 for $\bar{\eta} = 3.624$ where the contour "breaks" into upper and lower branches.

What this suggests is that experiments can easily measure values of $\bar{\eta}$ up to about 3.6. This value, however, represents only a slight increase over the Newtonian value of 3.0, and thus it would be difficult to accurately detect this difference with most experimental techniques. It is clear, therefore, that only experiments which produce very large gradients (either positive or negative) provide any real hope for a critical evaluation of the theoretical predictions for $\bar{\eta}$. Moreover, Figure 1 indicates that this gradient must be maintained for a minimum length of time. Consider, for example, a stretching rate of 1000 sec^{-1} imposed on the solution shown in Figure 1. Since $\lambda_1 \approx 10^{-3} \text{ sec}$, $\bar{\eta}$ reaches 10^4 when t is 10^{-2} sec . Consequently, only measurements made after this time period will yield $\bar{\eta} \geq 10^4$. In order to reduce the value of t to $4 \times 10^{-3} \text{ sec}$, it is necessary to use $\Gamma = 2000 \text{ sec}^{-1}$. There is, therefore, a tradeoff between stretching rate and flow time. To illustrate the difficulties that arise from this situation, some general flow geometries will be considered.

ACCELERATING FLOWS ($\Gamma > 0$)

An easy way to generate an accelerating flow is to drive fluid through a nozzle. Consider the ideal case of a converging flow along the x axis as shown in Figure 2. Simple one-dimensional analysis assumes that the velocity component in the positive x direction is independent of y and z . If the flow rate Q is constant and $A(x)$ is the cross-sectional area, the x component of the velocity is

$$V(x) = \begin{cases} V_I, & x_0 \leq x \\ Q/A(x), & x_0 \leq x \leq 0 \\ V_F, & 0 \leq x \end{cases} \quad (6)$$

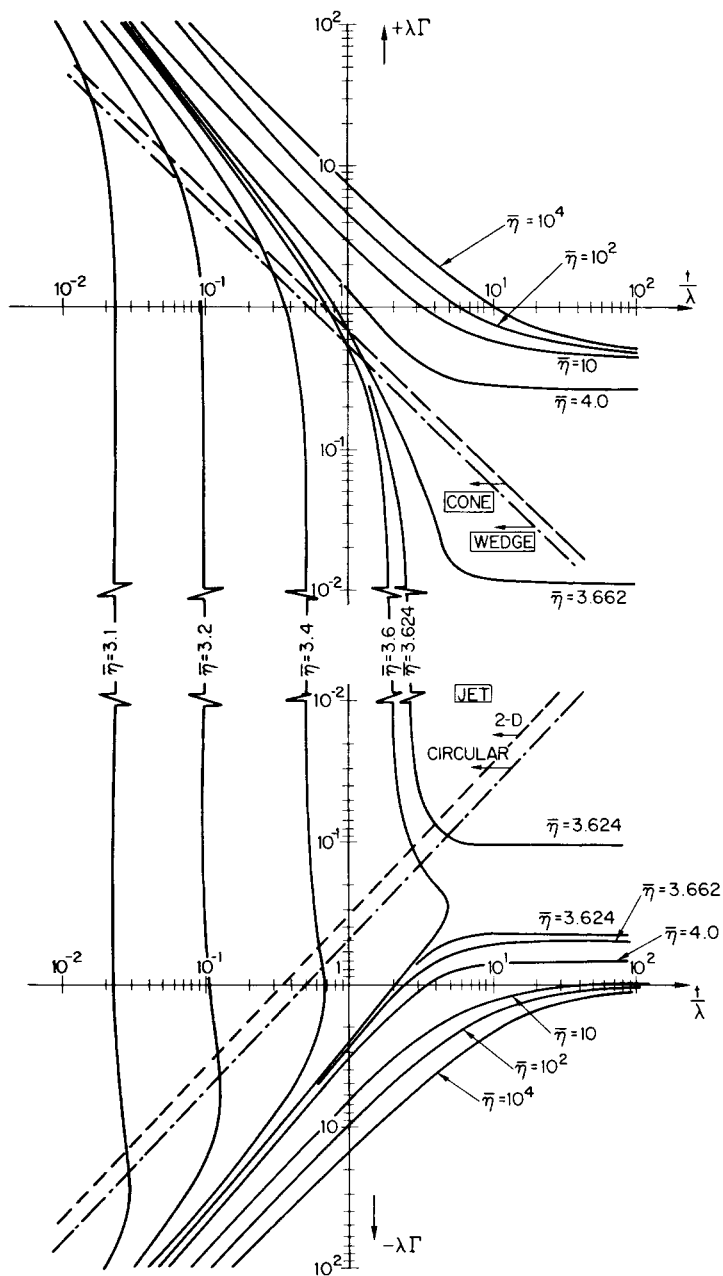


Fig. 1. Contours of constant $\bar{\eta}$ plotted in a phase plane of normalized stretching rate $\lambda_1 \Gamma$ and normalized flow time (t/λ_1). Limiting flow conditions obtainable in both accelerating and decelerating flows are given as straight dashed lines.

The stretching rate is

$$\Gamma = \frac{dV}{dx} = \frac{Q}{A^2} \frac{dA}{dx} \tag{7}$$

and the flow time is

$$t = \int_x^0 \frac{dx}{V(x)} = \frac{1}{Q} \int_x^0 A(x) dx \tag{8}$$

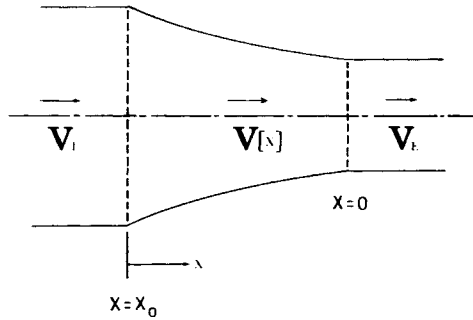


Fig. 2. Converging flow through a nozzle.

Now, the tradeoff between these two parameters, t and Γ , may be analyzed for two practical laboratory designs:

A. For a circular cone with radius $r(x) = b - cx$, the cross-sectional area is $A(x) = \pi[r(x)]^2$. The stretching rate may be calculated according to eq. (7),

$$\Gamma(x) = \frac{2cQ}{\pi(b - cx)^3}$$

which is an increasing function of x . If the stretching rate reaches a value $\Gamma = \Gamma_c$ at $x = x_c$, then the total flow time where $\Gamma > \Gamma_c$ (i.e., $x_c \leq x \leq 0$) is

$$t_c = \frac{1}{Q} \int_{x_c}^0 A(x) dx = \frac{2}{3\Gamma_c} - \frac{\pi b^3}{3cQ}$$

This, then, is the time available for experimental measurements of any increase in $\bar{\eta}$. Since t_c decreases with increasing b , it has an upper bound of

$$t_c = \frac{2}{3\Gamma_c} \quad (9)$$

B. Similarly, for a linear wedge with unit depth ($z = 1$) and a height of $y(x) = b - cx$, the stretching rate is

$$\Gamma(x) = \frac{Qc}{2(b - cx)^2}$$

The total flow time where $\Gamma \geq \Gamma_c$ is

$$t_c = \frac{1}{2\Gamma_c} - \frac{b^2}{cQ}$$

which is limited to values less than

$$t_c = \frac{1}{2\Gamma_c} \quad (10)$$

Both of these limiting conditions, eqs. (9) and (10), are shown in Figure 1 as straight dashed lines. Consequently, any laboratory setup which uses a cone- or wedge-shaped flow field can generate only $\Gamma - t$ combinations to the left of these straight lines which represent the upper limits on the flow conditions. While it is true that the convected Maxwell model gives only an approximate description for polymer solution behavior, the results shown in Figure 1 clearly indicate that the necessity to obtain minimum values for both Γ and t represents

a severe limitation. This limitation is an important factor for both cone and wedge flows.

To illustrate this point, a further example will be considered—flow through a two-dimensional hyperbolic wedge. If the cross-sectional area varies as $A(x) = 2b/(cx + 1)$ with unit depth, the nozzle exit ($x = 0$) has the area $A(0) = 2b$. The stretching rate is, therefore,

$$\Gamma(x) = Qc/2b = \text{constant}$$

and the flow time is

$$t = \frac{2b}{Qc} \ln \left[\frac{1}{cx + 1} \right]$$

For $\Gamma > \Gamma_c$, it can be shown that

$$t_c \Gamma_c = \ln \left[\frac{1}{cx_c + 1} \right] \quad (11)$$

Equation (11) represents a family of straight lines having a negative slope of unity in a log-log plot of the phase plane (Γ, t). The value of the parameter cx_c , therefore, determines the level of $\bar{\eta}$ that can be reached. Once this parameter is determined, however, it prescribes the shape and length of the hyperbolic nozzle which will give the maximum value of $\bar{\eta}$. The equations indicate that the cross-sectional area of the wedge must decrease by a factor of $(cx_c + 1)$ in a distance of x_c . If typical values of b or the exit cross section are selected, a simple calculation shows that the major limitation is one of three factors: the extremely short physical length of the nozzle, the small dimensions of the exit, or the enormous flow rates involved. Consequently, although wedge-shaped flows can readily achieve the combinations of Γ and t required to obtain large values of $\bar{\eta}$, it is still necessary to carefully consider the limitations imposed by physical dimensions when designing the experiment.

DECELERATING FLOWS ($\Gamma < 0$)

Similar considerations may be given to decelerating flows ($\Gamma < 0$), where the fluid elements experience compressional forces in the flow direction. A free jet is chosen for this discussion, since the flow leaving an orifice to form the jet exhibits a decaying velocity field. The fluid elements start from a high velocity region, the momentum is transformed into a pressure head and eventually the flow is brought to rest by fluid friction. For a two-dimensional turbulent jet of a Newtonian fluid, it has been calculated³¹ that the velocity in the positive x direction is

$$V(x) = Kx^{-1/2}$$

where K represents a combination of flow constants. Consequently, the longitudinal gradient is

$$\Gamma(x) = \frac{dV}{dx} = -\frac{K}{2}x^{-3/2} < 0$$

The flow time over the region ($\Gamma < \Gamma_c$) is

$$t_c = \int_{x_0}^{x_c} \frac{dx}{V} (x_c^{3/2} - x_0^{3/2}) < \frac{2}{3K} x_c^{3/2}$$

and a limiting condition is derived as

$$t_c = \frac{1}{3(-\Gamma_c)} \quad (12)$$

Similarly, for a circular jet,

$$V(x) \sim x^{-1}$$

which leads to a limiting condition

$$t_c = \frac{1}{2(-\Gamma_c)} \quad (13)$$

Both eqs. (12) and (13) are derived using the axial velocity distributions of Newtonian jets. The detail distribution in the non-Newtonian case of polymer solutions is not known. Experimental observations, however, seem to indicate that a certain degree of jet swelling is present.³ In that case some of the momentum carried by the jet is expelled to the transversed directions and the jet becomes thicker and shorter than the corresponding Newtonian jet. It may be expected, therefore, that the longitudinal gradient is not greatly affected, but the flow time is considerably shortened. This means that eqs. (12) and (13) represent upper bounds and are perhaps conservative estimates for the case of polymer solutions. Both these conditions are plotted in Figure 1 to show that the flow conditions available for measurements are limited to the left portion of the phase plane, where only low $\bar{\eta}$ values can be observed. This result is similar to what was found for accelerating flows, and thus significant increases in $\bar{\eta}$ can be obtained only when large negative values of Γ are coupled with sufficiently long flow times. Here again, although the model represents only an approximate description for solution behavior, the results indicate that the proper combination of Γ and t is difficult to obtain experimentally. Thus, careful design of the apparatus is essential in experiments of this type.

CONCLUSIONS

The recent recognition of the importance of elongational viscosity $\bar{\eta}$, both for its own sake and for its role in other phenomena, has inspired a number of attempts to experimentally measure $\bar{\eta}$ for dilute polymer solutions. In some of these experiments,^{24,25} the extension of the polymer molecules was found to be unexpectedly small and the values of $\bar{\eta}$ were very close to the Newtonian value of 3.0. In other cases,²¹⁻²³ large extensions were obtained and very high values of $\bar{\eta}$ were observed. Even in the latter cases, however, the dependence of $\bar{\eta}$ on the stretching rate Γ and polymer concentration were not always in agreement with theoretical predictions.¹⁴⁻¹⁷ The analysis presented here suggests that an important shortcoming in these experiments is the lack of control on flow time t . Even a very simple equation such as the convected Maxwell model indicates that the present experiments are in a range where the effects of flow time can be very important. It is concluded, therefore, that differences in t are a major reason for the wide variety of results that have been obtained in what appeared to be very similar experiments.

Two other factors may also contribute to the diversity of results. First, entrance and exit effects are not usually considered in these experiments, and yet

they may have significant implications. Second, nonlinear effects such as the conformation instability recently proposed by Peterlin³² could affect the results. The instability effects, for example, would reduce the magnitudes of the flow times and stretching rates required to obtain a given value of $\bar{\eta}$. It is likely that these nonlinear effects are vital to the acquisition of large elongational viscosities. Despite these complications, however, it is very important to design the experimental conditions so that the optimum combination of flow time and stretching rate can be obtained. It is hoped that the results presented here will provide valuable guidelines in this regard.

References

1. J. L. Lumley, *J. Polym. Sci., Macromol. Rev.*, **7**, 263 (1973).
2. K. A. Smith, G. H. Keuroghlian, P. S. Virk, and E. W. Merrill, *AIChE J.*, **15**, 294 (1969).
3. D. F. James and A. J. Acosta, *J. Fluid Mech.*, **42**, 269 (1972).
4. A. T. Ellis, J. G. Waugh, and R. Y. Ting, *J. Basic Eng.*, **92**, 459 (1970).
5. J. W. Hoyt, *Proc. 16th Amer. Towing Tank Conf.*, **1**, 7.0 (1971).
6. R. J. Hansen and D. L. Hunston, *J. Sound and Vibration*, **34**, 297 (1974).
7. R. J. Hansen and D. L. Hunston, *Proc. Eighth International Congress on Acoustics*, Goldcrest Press, London, 1974.
8. M. Gordon, J. Yerushalmi, and R. Shinnar, *Trans. Soc. Rheol.*, **17**, 303 (1973).
9. J. W. Hoyt, J. J. Taylor, and C. D. Runge, *J. Fluid Mech.*, **63**, 635 (1974).
10. S. J. Kline, H. T. Kim, and W. C. Reynolds, *J. Fluid Mech.*, **50**, 133 (1971).
11. E. R. Corino and R. S. Brodkey, *J. Fluid Mech.*, **37**, 1 (1969).
12. G. L. Donohue, W. G. Tiederman, and M. M. Reischman, *J. Fluid Mech.*, **56**, 559 (1972).
13. A. Peterlin, *Nature*, **227**, 598 (1970).
14. F. A. Seyer and A. B. Metzner, *AIChE J.*, **15**, 626 (1969).
15. J. L. Lumley, *Ann. Rev. Fluid Mech.*, **1**, 367 (1969).
16. J. L. Lumley, *Phys. Fluids*, **15**, 217 (1972).
17. A. E. Everage and R. J. Gordon, *AIChE J.*, **17**, 1257 (1971).
18. R. Y. Ting, *J. Appl. Polym. Sci.*, **16**, 3169 (1972).
19. D. L. Hunston and R. Y. Ting, *Trans. Soc. Rheol.*, **19**, 115 (1975).
20. J. L. Lumley, *Symposia Mathematica*, Vol. IX, Academic Press, New York, 1972, pp. 315-334.
21. A. B. Metzner and A. P. Metzner, *Rheol. Acta*, **9**, 174 (1970).
22. R. Bragg and D. R. Oliver, *Nature, Phys. Sci.*, **241**, 131 (1973).
23. M. R. Mackley and A. Keller, *Roy. Soc. London, Phil. Trans.*, **A278**, 29 (1975).
24. K. A. Smith, E. W. Merrill, and H. Banijamali, *Proc. Int. Symp. Polymers and Lubrication*, CNRS, Brest, 1975, p. 341.
25. D. L. Hunston and R. Y. Ting, unpublished results.
26. P. E. Rouse, *J. Chem. Phys.*, **21**, 1272 (1953).
27. A. Peterlin, *Pure Appl. Chem.*, **12**, 563 (1966).
28. M. M. Denn and G. Marrucci, *AIChE J.*, **17**, 101 (1971).
29. J. G. Oldroyd, *Proc. Roy. Soc. (London)*, **A200**, 523 (1950).
30. F. T. Trouton, *Proc. Roy. Soc. (London)*, **A71**, 426 (1906).
31. H. Schlichting, *Boundary Layer Theory*, McGraw-Hill, New York, 1960, Chap. 23.
32. A. Peterlin, *Makromol. Chem.*, Suppl. 1, 453 (1975).

Received April 21, 1976

Revised May 20, 1976